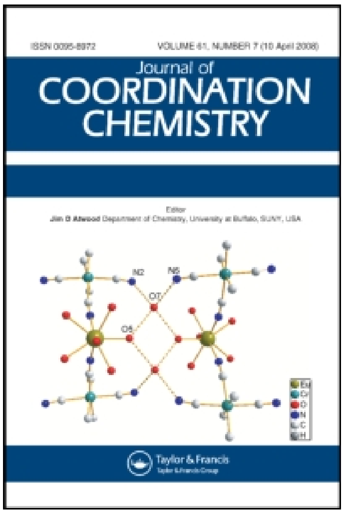

Journal of Coordination Chemistry

Publication details, including instructions for authors and subscription information:
http://www.informaworld.com/smpp/title~content=t713455674

Syntheses, crystal structures and magnetic properties of two cyano-bridged copper(I)-copper(II) mixed-valence complexes

Yi Jin[a]; Yunxia Che[a]; Jimin Zheng[a]
[a] Department of Chemistry, Nankai University 300071, Tianjin, P.R. China

To cite this Article Jin, Yi , Che, Yunxia and Zheng, Jimin(2006) 'Syntheses, crystal structures and magnetic properties of two cyano-bridged copper(I)-copper(II) mixed-valence complexes', Journal of Coordination Chemistry, 59: 6, 691 — 698

To link to this Article: DOI: 10.1080/00958970500364480

URL: http://dx.doi.org/10.1080/00958970500364480

Journal of Coordination Chemistry
Vol. 59, No. 6, 15 April 2006, 691–698

Syntheses, crystal structures and magnetic properties of two cyano-bridged copper(I)–copper(II) mixed-valence complexes

YI JIN, YUNXIA CHE and JIMIN ZHENG*

Department of Chemistry, Nankai University 300071, Tianjin, P.R. China

(*Received in final form 16 June 2005*)

Two cyano-bridged copper(II)–copper(I) mixed-valence assemblies, $Cu(EAM)_2[Cu(CN)_2]_2$ **1** (EAM = ethanolamine) and $Cu(DETA)[Cu(CN)_2]_2 \cdot 0.5H_2O$ **2** (DETA = diethylenetriamine), have been prepared and structurally and magnetically characterized. IR spectra indicate the presence of bridging cyano groups in both **1** and **2**, confirmed by structure analyses; Cu(I)–CN–Cu(II), Cu(I)–CN–Cu(I) and Cu(I)–Cu(I) metal bond linkages are evident. In the lattice, a 3D network is formed by two $[Cu(CN)_2]^-$ units and one $[Cu(EAM)_2]^{2+}$unit for **1**. Variable temperature magnetic susceptibilities, measured in the 5–300 K range, indicate weak antiferromagnetic exchange interactions in complex **1**.

Keywords: Mixed-valence; Cyanide; Ethanolamine; Diethylenetriamine; Crystal structure; Magnetic properties

1. Introduction

Much research interest has been focussed on the crystal engineering of metal coordination polymers [1–4]. Rational design of these polymeric structures has important implications for the development of new functional materials with potential applications such as zeolite-like materials, molecular selection, ion exchange, electrical conductivity, catalysis, and novel magnetic materials [5–15]. The chemistry of cyano-bridged coordination polymers is of current interest due to the remarkable diversity of structural types occurring in these systems, especially with bimetallic assemblies of Prussian Blue analogues, which exhibit unusual magnetic and electrical properties [16–23]. Copper(I)–copper(II) mixed-valence cyano-bridged compounds are of great biological importance and possess interesting electronic properties, [24–30]. In $[Cu(en)_2(H_2O)][Cu_2(CN)_4]$ [24], half of the cavities are occupied by $[Cu(en)_2(H_2O)]^{2+}$ cations acting as both template and guest; in $[Cu(pn)_2][Cu_2(CN)_4]$ [25], half of the cavities are occupied by $[Cu(pn)_2]^{2+}$ cations acting as template and the cavities

---

*Corresponding author. Email: jmzheng@public.tpt.tj.cn

Journal of Coordination Chemistry
ISSN 0095-8972 print: ISSN 1029-0389 online © 2006 Taylor & Francis
DOI: 10.1080/00958970500364480

are larger than those associated with $[Cu(en)_2(H_2O)]^{2+}$. Here we report two novel copper(I)–copper(II) mixed-valence cyano-bridged complexes, $Cu(EAM)_2[Cu(CN)_2]_2$ (**1**) (EAM = ethanolamine) and $Cu(DETA)[Cu(CN)_2]_2 \cdot 0.5H_2O$ (**2**) (DETA = diethylenetriamine). These possess a 3D network structure extended by the Cu(I)–CN–Cu(II), Cu(I)–CN–Cu(I) and Cu(I)–Cu(I) linkages, and complex **1** exhibits weak antiferromagnetic exchange interactions.

It is well-known that in aqueous solution copper(II) is easily reduced to copper(I) by cyanide. We have previously used aqueous solutions of $CuCl_2$ and $K_3[Cr(CN)_6]$ to grow cyano-bridged complexes $YM[Cr(CN)_6] \cdot H_2O$ by evaporation of solvent or by slow diffusion in a gel medium. When superfluous EAM solution or DETA are present in solution, complexes **1** and **2** are obtained, respectively. These represent unexpected hybrid Prussian Blue analogues.

2. Experimental

2.1. *Physical measurements*

Elemental analyses (C, H, N) were carried out with an Elementar Vario EL instrument. Infrared spectra (KBr pellets) were measured on a MAGNA-IR 560 FTIR spectrometer in the $400-4000\,cm^{-1}$ region. Magnetic studies were performed on MPMS SQUID and Maglab 2000 magnetometers in the temperature range 5–300 K.

2.2. *Syntheses*

2.2.1. $Cu(EAM)_2[Cu(CN)_2]_2$ (1). An aqueous solution containing $CuCl_2 \cdot 2H_2O$ (0.003 mmol) and ethanolamine (0.012 mmol) was added to an aqueous solution of $K_3[Cr(CN)_6]$ (0.002 mmol). Small black single crystals of **1** were obtained by slow evaporation during two weeks. The presence of excess EAM plays an important role in the decomposition of $K_3[Cr(CN)_6]$, to give CN^-, which partly reduces Cu(II) and complexes Cu(I). IR spectra show $\nu_{C\equiv N}$ at $2128\,cm^{-1}$ (Cu^I–CN). Anal. Calcd for **1** (%): C, 23.16; N, 20.26; H, 2.91; Cu, 45.95. Found: C, 23.17; N, 20.28; H, 2.89; Cu, 45.93.

2.2.2. $Cu(DETA)[Cu(CN)_2]_2 \cdot 0.5H_2O$ (2). Small black-green single crystals of **2** were obtained by slow diffusion over three weeks in a gel medium of an aqueous $CuCl_2$ solution into an aqueous solution containing $K_3[Cr(CN)_6]$ and DETA (1 : 1 : 1 mmol). The crystals were collected at the pump, washed with H_2O and MeOH, and air dried. DETA also plays an important role in the decomposition of $K_3[Cr(CN)_6]$. IR spectra show $\nu_{C\equiv N}$ at $2108\,cm^{-1}$ (CN–Cu^{II}). Anal. Calcd for **2** (%): C, 23.16; H, 2.92; N, 20.26; Cu, 45.95. Found: C, 23.15; H, 2.94; N, 20.25; Cu, 45.95.

2.3. *X-ray crystallography*

Diffraction data for **1** and **2** were collected at 293 K with a Bruker SMART 1000 CCD diffractometer using Mo-Kα radiation ($\lambda = 0.71073$ Å) with the ω–2θ scan technique. An empirical absorption correction (SADABS) was applied to raw intensities [31].

Table 1. Crystallographic data for **1** and **2**.

	1	**2**
Formula	$C_8H_{12}Cu_3N_6O_2$	$C_8H_{14}Cu_3N_7O_{0.50}$
Formula weight	414.86	406.88
Crystal system	Monoclinic	Orthorhombic
Space group	*C*2/*m*	*Pbcm*
a (Å)	9.384(2)	6.7841(11)
b (Å)	8.826(2)	16.512(3)
c (Å)	9.541(3)	24.084(4)
β (°)	117.305(5)	
V (Å^3)	702.2(3)	2698.0(8)
Z	2	8
D_c (g cm^{-3})	1.962	2.003
μ (mm^{-1})	4.507	4.683
Crystal size (mm)	0.14 × 0.12 × 0.10	0.20 × 0.16 × 0.10
θ range (°)	$2.40 < \theta < 25.02$	$1.69 < \theta < 25.01$
Reflections measured	1859	13,063
Independent reflections (R_{int})	672 (0.0473)	2426 (0.0771)
R_1, wR_2	0.0275, 0.0647	0.0456, 0.1029
Goodness-of-fit	1.084	1.045

Table 2. Selected bond lengths (Å) and angles (°) for **1**.

Bond lengths			
Cu(1)–N(1)	1.965(4)	Cu(1)–N(3)	2.041(6)
Cu(2)–C(1)	1.929(4)	Cu(2)–N(2)	1.951(3)
N(1)–C(1)	1.147(6)	N(3)–C(3)	1.494(7)
O(1)–C(4)	1.424(8)	C(3)–C(4)	1.525(7)
Cu(2)–Cu(2A)	2.7829(11)		
Bond angles			
N(1)–Cu(1)–N(3)	91.1(3)	C(1)–Cu(2)–N(2)	118.30(8)
C(1)–N(1)–Cu(1)	178.7(4)	N(1)–C(1)–Cu(2)	173.6(4)
C(3)–N(3)–Cu(1)	114.5(6)	N(3)–C(3)–C(4)	105.1(6)
O(1)–C(4)–C(3)	112.4(6)		

Unit cell parameters were obtained by least-squares refinement of setting angles of 1859 reflections with $2.40 < \theta < 25.02°$ for **1**, and of 13063 reflections with $1.69 < \theta < 25.01°$ for **2**. The structures were solved by direct methods and refined by full-matrix least-squares techniques based on F^2 with the SHELXTL program package [32]. Non-hydrogen atoms were refined anisotropically. Hydrogen atom positions were calculated theoretically. Weighting schemes used were $\omega = 1/[\sigma^2(F_o^2) + (0.0345P)^2 + 0.4010P]$ (**1**) and $\omega = 1/[\sigma^2(F_o^2) + (0.0521P)^2 + 8.9355P]$ (**2**), where $P = (F_o^2 + 2F_c^2)/3$. Crystallographic data are summarized in table 1 and selected bond lengths and angles are listed in tables 2 and 3.

3. Results and discussion

3.1. *Crystal structures*

The crystal structure analyses reveal that **1** and **2** consist of 3D polymers $\{Cu(EAM)_2[Cu(CN)_2]_2\}_n$ and $\{Cu(DETA)[Cu(CN)_2]_2 \cdot 0.5H_2O\}_n$, respectively. As shown in figure 1,

Table 3. Selected bond lengths (Å) and angles (°) for **2**.

Bond lengths			
Cu(1)–N(2)	1.960(11)	Cu(1)–N(1)	1.999(7)
Cu(1)–N(1A)	1.999(7)	Cu(1)–N(3)	2.085(7)
Cu(2)–N(9)	1.738(11)	Cu(2)–N(7)	1.785(8)
Cu(2)–N(8)	2.033(12)	Cu(2)–N(10)	2.053(8)
Cu(3)–C(3)	1.908(8)	Cu(3)–C(4)	1.950(6)
Cu(3)–C(5)	1.963(6)	Cu(3)–Cu(4)	2.8687(14)
Cu(4)–C(7)	1.937(10)	Cu(4)–C(6)	1.948(7)
C(1)–N(1)	1.331(11)	C(1)–C(2)	1.449(12)
C(3)–N(3)	1.134(9)	C(4)–N(4)	1.142(8)
C(7)–N(7)	1.140(10)	N(8)–C(8)	1.413(15)
C(8)–C(9)	1.627(18)	C(9)–N(9)	1.486(18)
N(9)–C(11)	1.451(18)	C(10)–N(10)	1.356(16)
C(10–C(11)	1.758(18)		
Bond angles			
N(2)–Cu(1)–N(1)	79.9(4)	N(2)–Cu(1)–N(3)	143.1(4)
N(1)–Cu(1)–N(3)	96.7(3)	N(7)–Cu(2)–N(9)	137.8(4)
N(7)–Cu(2)–N(8)	113.1(4)	N(9)–Cu(2)–N(8)	71.2(4)
N(7)–Cu(2)–N(10)	100.9(3)	N(9)–Cu(2)–N(10)	80.1(4)
N(8)–Cu(2)–N(10)	163.2(4)	C(3)–Cu(3)–C(4)	122.2(3)
C(3)–Cu(3)–C(5)	124.3(3)	C(4)–Cu(3)–C(5)	108.9(3)
C(3)–Cu(3)–Cu(4)	64.4(2)	C(4)–Cu(3)–Cu(4)	113.5(2)
C(5)–Cu(3)–Cu(4)	115.0(2)	C(7)–Cu(4)–C(6)	112.6(3)
C(7)–Cu(4)–Cu(3)	65.7(3)	C(6)–Cu(4)–Cu(3)	104.9(2)

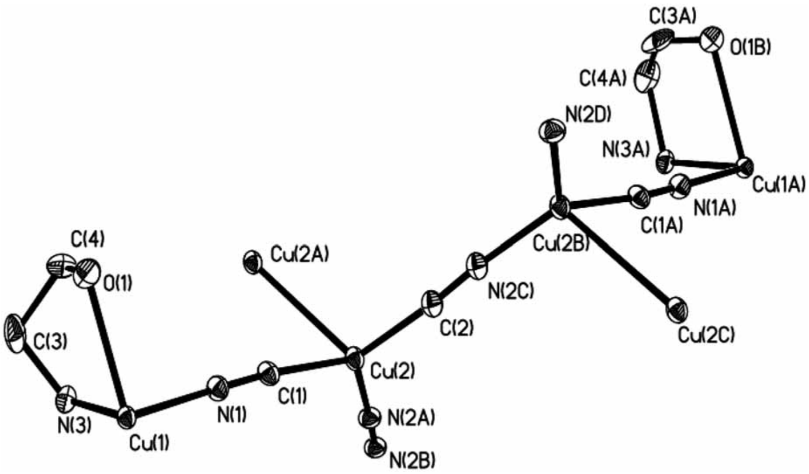

Figure 1. An ORTEP drawing of complex **1** showing the atom numbering scheme. Hydrogen atoms are omitted for clarity.

the asymmetric unit of **1** consists of two $[Cu(CN)_2]^-$ units and one $[Cu(EAM)_2]^{2+}$ unit. Each Cu(I) atom connects with three others and one Cu(II) ion to form a distorted tetrahedron. In this environment, Cu(I) links to other two Cu(I) ions and one Cu(II) ion through cyano-bridges and Cu(I) links to Cu(II) ion through another CN^- bridge [Cu(I)–C = 1.929(4) Å, N–Cu(II) = 1.965(4) Å, and C(I)–N(1) = 1.147(6) Å]; the Cu(I)–Cu(I) links involve disordered cyano-bridges with 50% C and N occupancies

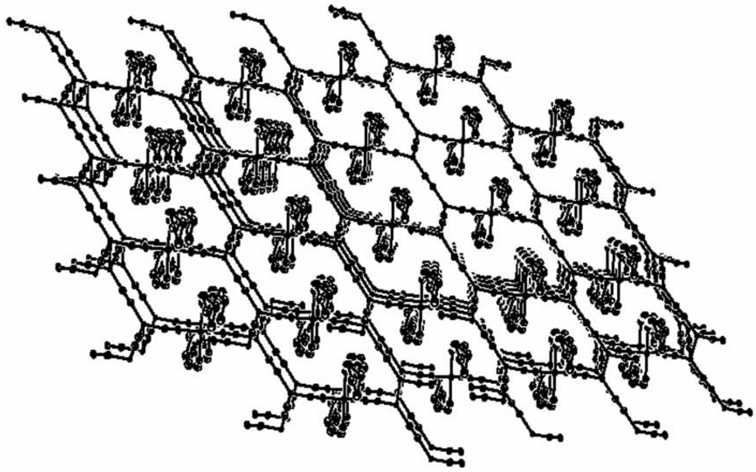

Figure 2. The three-dimensional network structure of complex **1**.

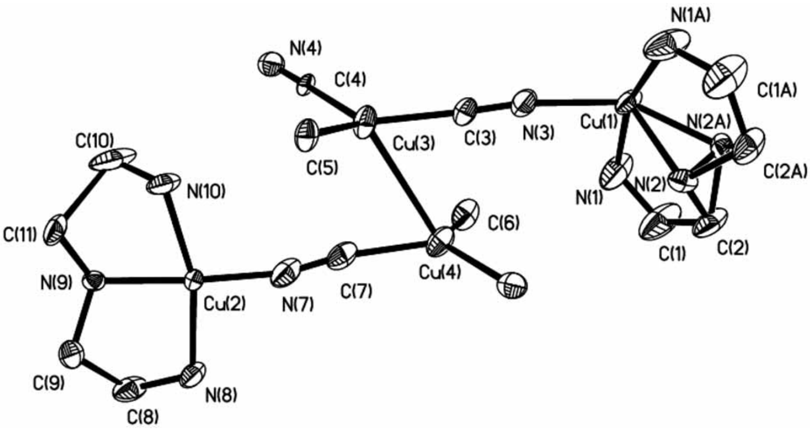

Figure 3. An ORTEP drawing of complex **2** showing the atom numbering scheme. The H_2O molecule and hydrogen atoms are omitted for clarity.

(C2/N2′ and N2/C2′ bond distances are 1.148(18) Å). An additional Cu(I)–Cu(I) metal bond (2.783 Å) is involved in bridging. Each Cu(II) ion exhibits distorted octahedral coordination, with two nitrogen and two oxygen atoms of two EAM molecules in the equatorial plane [Cu–N = 2.041(6) Å] and two cyano nitrogen atoms in axial positions [Cu–N = 1.965(4) Å]. The nitrogen and oxygen atoms of EAM are also disordered. In the lattice, a 3D network structure is formed by two $[Cu(CN)_2]^-$ units and one $[Cu(EAM)_2]^{2+}$ unit (figure 2). Adjacent Cu(I)–CN–Cu(II) and Cu(I)–CN–Cu(I) fragments are 5.030 and 5.050 Å apart, respectively. The network comprises a regular grid with six Cu(I) atoms surfaces parallel to the *ac* plane and at two centers, and ten Cu(II) atoms on surfaces parallel to the *ab* plane and on eight edges.

The asymmetric unit of **2** is composed of one $[Cu(DETA)]^{2+}$ unit, two $[Cu(CN)_2]^-$ units and one H_2O molecule (figure 3). Each Cu(I) ion lies in a distorted tetrahedral

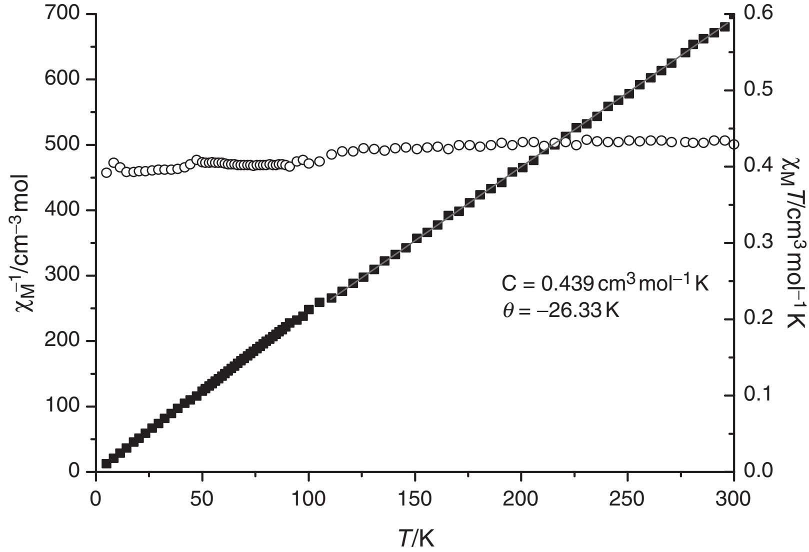

Figure 4. Plots of χ_M^{-1} and χ_MT *vs.* T per Cu(II)Cu(I)$_2$ unit for **1**.

environment, and connect to one [Cu(DETA)]$^{2+}$ unit and one Cu(I) ion through ordered CN$^-$ bridges. Other cyano ligands link another Cu(I) ion with disordered CN$^-$ bridges, and the framework is completed by a Cu(I)–Cu(I) bond (2.869(2) Å). The Cu(II) atom Cu(1) is five-coordinate, with two cyano nitrogen atoms of different [Cu(CN)$_2$]$^-$ units and three nitrogen atoms of DETA being bonded. In DETA, the N(2) atom is disordered. The Cu(II) atom Cu(2) is also five-coordinate, with two cyano nitrogen atoms of two different [Cu(CN)$_2$]$^-$ units and three nitrogen atoms DETA molecule bonding; in the DETA molecular, Cu(2), C(9), C(11), N(8), N(9) are disordered. The O1 atom of the H$_2$O molecule is also disordered. Adjacent Cu(I)–CN–Cu(II) distances are 4.843 to 5.107 Å and adjacent Cu(I)–CN–Cu(I) distances 5.048 Å. The resulting 3D network is formed by a regular array of two [Cu(CN)$_2$]$^-$ units and one [Cu(DETA)]$^{2+}$ unit.

3.2. *Magnetic properties*

A χ_M versus T plot for **1** over the temperature range of 5–300 K (figure 4), in which χ_M is the corrected magnetic susceptibility per Cu(II)Cu(I)$_2$ unit, can be fitted to the Curie–Weiss law $\chi_M = C/(T - \theta)$ above 109 K, giving a Curie constant $C = 0.439\,\text{cm}^3\,\text{mol}^{-1}\,\text{K}$, and a Weiss constant $\theta = -26.33$ K. The C value is slightly higher than the expected value $0.375\,\text{cm}^3\,\text{mol}^{-1}\,\text{K}$ for one Cu(II) ($S = 1/2$) ion and two Cu(I) ($S = 0$) ions. This behaviour could be justified on the basis of the sum of contributions arising from the purely ground-state configuration of Cu(II) and the one mediated by the CN–Cu(I)–CN bridge. The negative value of θ indicates weak antiferromagnetic exchange. The χ_M value of $0.430\,\text{cm}^3\,\text{mol}^{-1}$ at room temperature decreases with decreasing temperature to $0.393\,\text{cm}^3\,\text{mol}^{-1}$ at 5 K. The magnetic behaviour of **2** is different (figure 5), with χ_M decreasing with

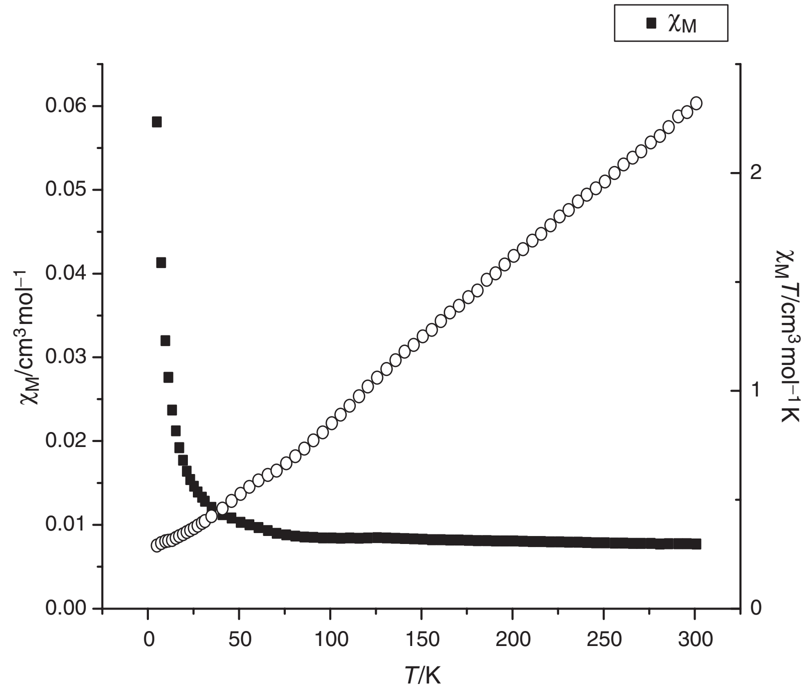

Figure 5. Plots of χ_M and $\chi_M T$ *vs.* T per Cu(II)Cu(I)$_2$ unit for **2**.

decreasing temperature; the χ_M value per Cu(II)Cu(I)$_2$ unit could not be fitted to the Curie–Weiss law.

Supplementary material

Crystallographic data (excluding structure factors) have been deposited with the Cambridge Crystallographic Data Centre as supplementary publications 284089 ($Cu(EAM)_2[Cu(CN)_2]_2$) and CCDC 284090 ($Cu(DETA)[Cu(CN)_2]_2 \cdot 0.5H_2O$). Copies of the data can be obtained free of charge on application to CCDC, 12 Union Road, Cambridge, CB2 1EZ, UK (Fax: (+44) 1223 336-033; E-mail: deposit@ccdc.cam.ac.uk).

Acknowledgements

This work was supported by the National Natural Science Foundation of China (No. 50572040).

References

[1] R. Robson, B.F. Abraham, S.R. Batten, R.W. Gable, B.F. Hoskins, J. Liu. In *Supramolecular Architecture*, T. Bein (Ed.), Chapter 19, p. 258, American Chemical Society, Washington (1992); (R. Robson. *Comprehensive Supramolecular Chemistry*, Chapter 22, p. 733, Pergamon Press,

New York (1996)), K.R Seddon, M.J. Zaworotko (Eds), *Crystals Engineering: The Design and Applications of Functional Solids*, Kluwer Academic Publishers, Dordrecht, The Netherlands (1999).
[2] M.J. Zaworotko. *Angew. Chem., Int. Ed.*, **39**, 3052 (2000**)**.
[3] S. Kitagawa, M. Kondo. *Bull. Chem. Soc. Jpn.*, **71**, 1739 (1998).
[4] A.J. Blake, N.R. Champness, P. Hubberstey, W.S. Li, M.A. Withersby, M. Schröder. *Coord. Chem. Rev.*, **183**, 117 (1999).
[5] O.M. Yaghi, G. Li, H. Li. *Nature*, **378**, 703 (1995).
[6] O.M. Yaghi, H. Li, T.L. Groy. *J. Am. Chem. Soc.*, **118**, 9096 (1996).
[7] O.M.Yaghi, H. Li. *J. Am. Chem. Soc.*, **117**, 10401 (1995).
[8] O.M. Yaghi, H. Li. *J. Am. Chem. Soc.*, **118**, 295 (1996).
[9] H. Li, M. Eddaoudi, M. O'Keefe, O.M. Yaghi. *Nature*, **402**, 276 (1999).
[10] M. Kondo, T. Okubo, A. Asami, S. Noro, T. Yoshimoto, S. Kitagawa, T. Ishii, H. Matsuzaka, K. Seki. *Angew. Chem., Int. Ed.*, **38**, 140 (1999).
[11] M. Fujita, Y.J. Kwon, S. Washizu, K. Ogura. *J. Am. Chem. Soc.*, **116**, 1151 (1994).
[12] M. Kondo, T. Yoshimoti, K. Seki, H. Matsuzaka, S. Kitagawa. *Angew. Chem., Int. Ed.*, **36**, 1725 (1997).
[13] S. Noro, S. Kitagawa, M. Kondo, K. Seki. *Angew. Chem., Int. Ed.*, **39**, 2082 (2000).
[14] O. Kahn (Ed.). *Magnetism: A Supramolecular Function*, Kluwer Academic Publishers, Dordrecht, The Nederlands (1996); E. Coronado, P. Delhaes, D. Gatteschi, J.S. Miller (Eds), M*olecular Magnetism: From the Molecular Assemblies to the Devices*, pp. 43, 179, Kluwer Academic Publishers, Dordrecht, The Netherlands (1996).
[15] E. Coronado, J.R. Galan-Mascaros, C.J. Gomez-Garcıa, V. Laukhin. *Nature*, **408**, 447 (2000).
[16] J.S. Miller, A.J. Epstein. *Angew. Chem. Int. Ed. Engl.*, **33**, 385 (1994).
[17] O. Kahn. *Molecular Magnetism*, VCH, New York (1993).
[18] D. Gatteschi, O. Kahn, J.S. Miller, F. Palacio (Eds). *Magnetic Molecular Materials*, Kluwer Academic Publishers, Dordrecht, The Netherlands (1991).
[19] H.O. Stumpf, L. Ouahab, Y. Pel, P. Bergerat, O. Kahn. *J. Am. Chem. Soc.*, **116**, 3866 (1994).
[20] O. Kahn. *Nature*, **378**, 667 (1995).
[21] S.M. Holmes, G.S. Girolami. *J. Am. Chem. Soc.*, **121**, 5593 (1999).
[22] H.Z. Kou, S. Gao, J. Zhang, G.H. Wen, G. Su, R.K. Zhang, X.X. Zhang. *J. Am. Chem. Soc.*, **123**, 11809 (2001).
[23] W. Dong, L.N. Zhu, H.B. Song, D.Z. Liao, Z.H. Jiang, S.P. Yan, P. Cheng, S. Gao. *Inorg. Chem.*, **43**, 2465 (2004).
[24] R.J. Williams, A.C. Larson, D.T. Cromer. *Acta Crystallogr.*, **B28**, 858 (1972).
[25] E. Colacio, R. Kivekas, F. Lloret, M. Sunberg, J. Suarez-Varela, M. Bardaji, A. Laguna. *Inorg. Chem.*, **41**, 5141 (2002).
[26] D.D. Le Cloux, R. Davydov, S.J. Lippard. *J. Am. Chem. Soc.*, **120**, 6810 (1998).
[27] R.P. House, V.G. Young, W.B. Tolman. *J. Am. Chem. Soc.*, **118**, 2101 (1996).
[28] D.R. Gamelin, K.R. Williams, L.B. La Croix, R.P. Houser, W.B. Tolman, T.C. Mulder, S. de Vries, B. Hedman, K.O. Hodgson, E.I. Solomon. *J. Am. Chem. Soc.*, **119**, 613 (1997).
[29] S.D. George, M. Metz, R.K. Szilagyi, H. Wang, S.P. Cramer, Y. Lu, W.B. Tolman, B. Hedman, K.O. Hodgson, E.I. Solomon. *J. Am. Chem. Soc.*, **123**, 5757 (2001).
[30] J.-M. Zheng, S.R. Batten, M. Du. *Inorg. Chem.*, **44**, 3371 (2005).
[31] G.M. Sheldrick. *SADABS: Program for Empirical Absorption Correction of Area Detector Data*, University of Göttingen, Germany (1996).
[32] G.M. Sheldrick. *SHELXTL: Structure Determination Software Programs*, Bruker Analytical X-ray Systems, Inc., Madison, WI (1997).